

1 Article

2 Isomerization of Glucose to Fructose in Hydrolyzates 3 from Lignocellulosic Biomass using Hydrotalcite

4 David Steinbach ^{1,*}, Andreas Klier ¹, Andrea Kruse ², Jörg Sauer ¹, Stefan Wild ¹ and
5 Marina Zanker ¹

6 ¹ Karlsruhe Institute of Technology (KIT), Institute for Catalysis Research and Technology, Hermann-von-
7 Helmholtz-Platz 1, 76344 Eggenstein-Leopoldshafen, Germany; j.sauer@kit.edu

8 ² University of Hohenheim, Institute of Agricultural Engineering, Garbenstrasse 9, 70599 Stuttgart,
9 Germany; Andrea_Kruse@uni-hohenheim.de

10 * Correspondence: David.Steinbach@partner.kit.edu

11 Received: date; Accepted: date; Published: date

12 **Abstract:** The isomerization of glucose-containing hydrolyzates to fructose is a key step in the
13 process from lignocellulosic biomass to the platform chemical hydroxymethylfurfural. We
14 investigate the isomerization reaction of glucose to fructose in water catalyzed by hydrotalcite.
15 Catalyst characterization is performed via IR, XRD and SEM. Firstly, glucose solutions at pH-neutral
16 conditions are converted under variation of temperature, residence time and catalyst loading
17 whereby a maximum of 25 wt.% fructose yield is obtained at 38 wt.% glucose conversion. Secondly,
18 isomerization is performed at $pH=2$ using glucose solutions as well as glucose-containing
19 hydrolyzates from lignocellulosic biomass. Under acidic conditions, the hydrotalcite loses its
20 activity for isomerization. In consequence, it is unavoidable to neutralize the acidic hydrolyzate
21 before the isomerization step with an inexpensive base. As a neutralizing agent NaOH is preferred
22 over $Ba(OH)_2$, since higher fructose yields are achieved with NaOH. Last, a pH-neutral hydrolyzate
23 from lignocellulose is subjected to isomerization, yielding 16 wt.% fructose at 32 wt.% glucose
24 conversion. This work targets the application of catalytic systems on real biomass-derived samples.

25 **Keywords:** glucose; fructose; aldose-ketose isomerization; pretreatment; hydrolyzate;
26 lignocellulose; hydrotalcite; hydroxymethylfurfural; biorefinery; bioeconomy
27

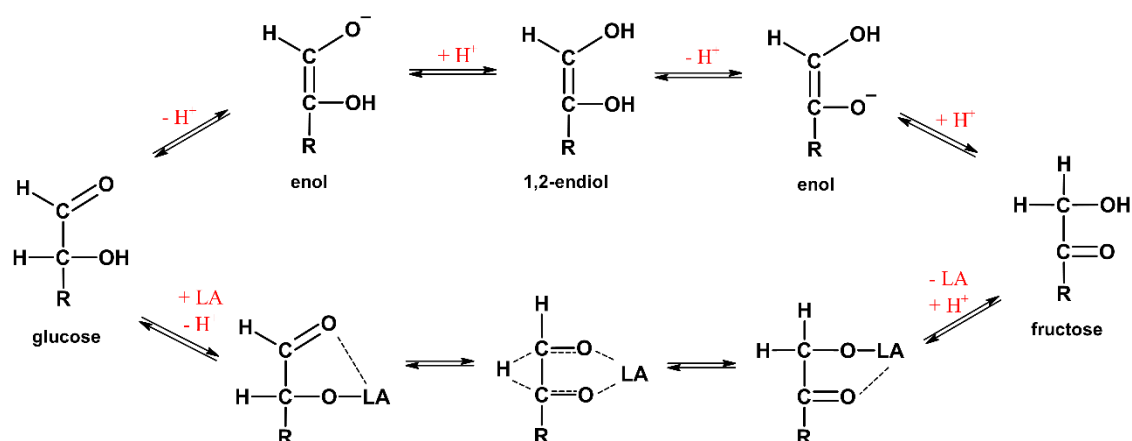
28 1. Introduction

29 Producing platform chemicals from renewable lignocellulose, which is considered as a second
30 generation biomass, has grown into a central point of interest. This is due to the limited availability
31 of fossil resources, coupled with the aim to reduce the carbon footprint of such products [1]. One
32 example is the production of hydroxymethylfurfural (HMF), which is one of the most important bio-
33 based building blocks and can be converted into a variety of interesting chemicals [2]. HMF can be
34 synthesized based on hexoses and their polymers, including lignocellulosic cellulose, which consists
35 of glucose units. However, low yields from direct conversion of glucose to HMF in aqueous media
36 are reported [2]. A previous isomerization of glucose to fructose could help to overcome this obstacle,
37 because under the same reaction conditions HMF yields from fructose are higher than those from
38 glucose [3].

39 The isomerization of glucose to fructose is carried out industrially with pH-neutral glucose
40 solutions [4], which have a higher glucose concentration than process waters from the acid-catalyzed
41 pretreatment of lignocellulose (hydrolyzates). In addition, the hydrolyzates are highly acidic and
42 contain numerous by-products. Due to these different properties with regard to pH value, by-
43 products and glucose concentration, a suitable isomerization catalyst for hydrolyzates has to be
44 experimentally investigated.

45 Glucose cannot be completely converted to fructose in a single step, because the thermodynamic
 46 equilibrium ratio between glucose to fructose at 25 °C is 54:46 [5]. At higher temperatures the
 47 equilibrium shifts towards fructose, caused by the weak endothermicity of the reaction (standard
 48 reaction enthalpy of 2.8 kJ/mol [5]).

49 The conversion of glucose to fructose is an aldose-ketose isomerization, which can take place via
 50 two mechanistic pathways (see Figure 1). The first pathway is a keto-enol tautomerism, which is
 51 called Lobry-de-Bruyn-van-Ekenstein rearrangement. This rearrangement is catalyzed by Brønsted
 52 bases as a proton acceptor and takes place via the 1,2-endiol. In a second mechanistic scenario, a
 53 Lewis acid is used, which also abstracts a proton and an intramolecular hydrogen shift follows. This
 54 hydrogen shift was demonstrated in a study by Román-Leshkov and co-workers [6] using a
 55 Sn-β zeolite as a Lewis acid. This zeolite also catalyzes the ring opening of glucose into the acyclic
 56 form of the sugar [7]. Also, for the biochemical isomerization an intramolecular hydrogen shift takes
 57 place [8,9], so that the enzyme participates in the reaction in a similar way as a Lewis acid.



58

59 **Figure 1.** Mechanistic scenarios for isomerization of glucose to fructose [6], Brønsted-base-catalyzed
 60 keto-enol tautomerism with hydrogen transfer (top) and Lewis acid-catalyzed intramolecular
 61 hydrogen shift (bottom), LA: Lewis acid

62 Even without the presence of a catalyst, glucose isomerizes to fructose in hot high-pressure
 63 water [10]. However, in this case the isomerization is a side reaction with low fructose selectivities,
 64 whereas other reactions predominate, like glucose defragmentation. In order to accelerate the glucose
 65 isomerization, various homogeneous and heterogeneous catalysts were investigated, which are
 66 summarized by Delidovich and Palkovits [11]. In all studies, glucose is used as a pure substance in
 67 aqueous solutions. To the best of our knowledge, the isomerization of a hydrolyzate from the
 68 pretreatment of lignocellulose has not yet been investigated.

69 Heterogeneous catalysts are promising because they can be separated easily from the liquid
 70 phase for catalyst recycling. Both Brønsted bases and Lewis acids can be applied as a heterogeneous
 71 catalyst. Investigated heterogeneous Brønsted bases for isomerization include magnesium oxide,
 72 zirconium carbonate, hydrotalcite, attapulgite, zeolites modified with alkali and alkaline earth
 73 metals, microporous metal silicates and basic resins [11,12]. An example for Lewis acid
 74 heterogeneous catalysts are the group of Sn-β zeolites. The metal oxides of zirconium and titanium
 75 occupy an intermediate position, because they have both Lewis acid sites and base sites and thus act
 76 as bifunctional catalysts [13].

77 The isomerization results using hydrotalcites are summarized in Table 1. Hydrotalcites are
 78 magnesium-aluminum-hydroxycarbonates that occur as natural minerals or can be produced
 79 synthetically. The general formula is $[Mg_{1-x}Al_x(OH)_2]^{x+}[A]^{x-} \cdot mH_2O$, where x is the molar fraction of
 80 aluminum in the metal content and A symbolizes the anions, which are typically present as CO_3^{2-} and
 81 OH. Hydrotalcite forms layered structures with positively charged metal hydroxide layers and
 82 intermediate layers containing water and anions [14]. The anions in the interlayers are considered to
 83 be the active site for the isomerization [11]. The important aspect is, whether the anions are present

84 as CO_3^{2-} or OH^- , since OH^- has a higher basicity and is therefore more catalytically active than CO_3^{2-}
 85 [11,15]. In addition, the accessibility of the catalytic anions plays a role in the isomerization, since
 86 glucose cannot penetrate into the intermediate layers of the hydrotalcite [11,16].

87 By calcining the hydrotalcite, first water is released from the intermediate layers and at higher
 88 temperatures CO_2 from the carbonate anions [15]. This creates a mixed $\text{MgO-Al}_2\text{O}_3$ metal oxide with
 89 a large surface area [11,17]. However, the mixed metal oxides can incorporate anions into the
 90 intermediate layer, which again results in hydrotalcite, which is known as memory effect [15,17].
 91 Rehydration with water causes OH^- anions, whereas CO_2 contact causes the formation of CO_3^{2-} anions
 92 in the intermediate layer [15]. The OH^- layer in the intermediate layer is not stable in the presence of
 93 air and is converted into the carbonate form by CO_2 absorption [16].

94 Yu et al. [17] investigated the influence of hydrotalcite calcination and rehydration on glucose
 95 isomerization. The calcined catalyst provided a high glucose conversion with poor fructose
 96 selectivity, which is caused by strongly basic sites of the mixed oxides [17]. On the other hand, the
 97 hydrotalcite rehydrated after calcination in water showed a high fructose selectivity, which is
 98 explained by weakly basic sites [17]. In a similar study by Delidovich and Palkovits [18], the
 99 hydrotalcite rehydrated in water gave the best fructose yields. A further work showed that targeted
 100 catalyst synthesis influences the basicity of the hydrotalcite [16]. A higher basicity not only leads to a
 101 higher glucose turnover, but also to a higher fructose yield [16]. Additionally, hydrotalcite can be
 102 regenerated by burning off organic deposits and rehydrating in water [16].

103 **Table 1.** Isomerization of glucose to fructose using hydrotalcite catalysts

temperature [°C]	reaction time [min]	glucose conversion [wt.%]	fructose selectivity [wt.%]	fructose yield [wt.%]	ref
90	60	28	78	22	[15]
90	120	41	75	31	[18]
110	180	34	89	30	[16]
95	?	42	60	25	[19]
120	60	43	64	27	[20]
100	?	18	78	14	[21]
90	120	61	83	50	[22]
100	300	27	74	20	[23]
100	300	61	70	42	[24]
100	180	38	66	25	[25]
120	240	36	75	27	[26]
100	300	54	56	30	[27]

104
 105 No investigated heterogeneous catalyst enables a completely selective conversion of glucose into
 106 fructose. By-products are formed which differ in species and yield, depending on the applied reaction
 107 conditions and used catalyst. Most studies report sugar epimer mannose as a by-product. Using
 108 hydrotalcite as catalyst, reported by-products of isomerization are dihydroxyacetone,
 109 glycolaldehyde, lactic acid and traces of glyceraldehyde [18]. The two C3 compounds
 110 dihydroxyacetone and glyceraldehyde are formed by adol splitting of fructose [28]. Glyceraldehyde
 111 can only be found in traces because it dehydrates to methylglyoxal, which is further converted into
 112 lactic acid in a benzylic acid rearrangement [28,29]. The pH value of the product liquid drops due to
 113 the produced lactic acid, which leads to the removal of Mg^{2+} ions from the hydrotalcite [18].

114 In this study, we investigate the isomerization reaction of glucose to fructose in water, using
 115 hydrotalcite as a catalyst. Firstly, glucose solutions at pH-neutral conditions are converted under
 116 variation of temperature, mass ratio of catalyst to glucose and reaction time. Thereby, the optimal
 117 reaction conditions for glucose isomerization are determined. Catalyst characterization is performed
 118 via IR, XRD and SEM. Secondly, isomerization is performed at pH-acidic conditions, using glucose
 119 solutions as well as glucose-containing hydrolyzates from lignocellulosic biomass. Thereby, the
 120 catalytic performance at pH-acidic conditions is investigated. Last, a pH-neutral hydrolyzate is

121 subjected to isomerization, in order to compare isomerization of lignocellulose-derived sample with
122 glucose solutions.

123 2. Materials and Methods

124 2.1. Obtaining a glucose-containing hydrolyzate from lignocellulosic biomass

125 An acid-catalyzed pretreatment of lignocellulose is performed to obtain a glucose-containing
126 hydrolyzate. Beech wood chips (Joh. Sinnerbrink, Verl, Germany) or spruce wood chips (Hermann
127 Keller, Achern, Germany) are used as educts. Diluted sulfuric acid is used as catalyst to hydrolyze
128 hemicelluloses and cellulose polymers in lignocellulose structure to water-soluble sugar monomers.

129 A semi-continuous test rig is used for pretreatment, where the liquid phase is continuously
130 exchanged [30]. This has the advantage that liberated water-soluble molecules like sugar monomers
131 are removed from the hot reactor and thus largely protected from secondary reactions. 180 and 200 °C
132 are used as reactor temperatures. The stainless-steel reactor has an internal volume of 100 ml and is
133 loaded with 15 g pre-dried wood chips as a fixed bed before the experiment. Demineralized water or
134 dilute acid solution is continuously feed into the reactor at a volume flow of 15 mL/min.
135 Demineralized water is pumped through the reactor during the heating phase. When the target
136 temperature in the reactor is reached, the feed stream is switched to 0.05 mol/L dilute sulfuric acid
137 solution. The hydrolyzate leaves the reactor continuously and is cooled in a heat exchanger.
138 Hydrolyzate sample is collected for about 1 hour acid-catalyzed lignocellulose hydrolysis and
139 afterwards stored at 4 °C until further processing. The main organic components in the hydrolyzate
140 of spruce wood are 2.1 g/L glucose, 0.91 g/L hydroxymethylfurfural, 0.23 g/L furfural, 0.05 g/L
141 levulinic acid, 0.03 g/L formic acid and 0.03 g/L acetic acid. Other sugars like mannose, xylose and
142 fructose as well as short-chain organic compounds and high-molecular-weight substances such as
143 humines are present in unknown quantities.

144 The hydrolyzates are neutralized to pH = 7 by adding a strong base. This is done with constant
145 stirring and pH measurement using a glass electrode. Concentrated sodium hydroxide or barium
146 hydroxide solutions are used as bases. After neutralization, the solution is filtered through a 0.45 µm
147 nylon membrane filter.

148 2.2. Isomerization experiments

149 The hydrotalcite catalyst in powder form with the formula $Mg_6Al_2[(OH)_{16}CO_3] \cdot 4H_2O$ was
150 purchased (Sigma-Aldrich, St. Louis, MO, USA). The calcination was performed in a muffle furnace
151 at 450 °C for 6 h with a continuous nitrogen purge. After the calcination, the catalyst is stored under
152 nitrogen inert gas.

153 The isomerization is carried out in a glass apparatus. A defined amount of the calcinated catalyst
154 and 40 ml of glucose solution or hydrolyzate are placed in a 100 ml three-neck bottom flask with a
155 magnetic stirrer. On top of the flask, a reflux cooler is installed and the flask is heated in a preheated
156 oil bath to the reaction temperature of 65 - 100 °C within about 20 min, whereby the reaction
157 temperature is measured in the solution. The gas phase in the glass apparatus was either air or inert
158 gas via continuously introducing nitrogen into a side neck. After the reaction time of 0-120 min has
159 passed, the flask is removed from the oil bath and cooled by ambient air, while stirring continues.
160 The content of the flask is then transferred quantitatively to a vacuum filtration unit and filtered
161 through a 0.45 µm nylon membrane. 20 ml of deionized water is added to the vacuum filtration unit,
162 to wash the filter cake.

163 When an error bar is shown in the following diagrams, the isomerization experiments were
164 carried out at least in triplicate, otherwise as a single determination. Fructose yield after isomerization
165 of hydrolysate is calculated based on glucose in hydrolyzate, not including other hexoses.

166 2.3. Analytics

167 Characterization of the liquid samples after isomerization was performed with several HPLC
168 methods. Preliminary filtration with 0.45 µm GHP syringe filters (Pall, New York, NY, USA) was

169 performed to remove high-molecular-weight products. Glucose, fructose and mannose were
170 separated at 35 °C in a Metrosep Carb 2 column (Metrohm, Filderstadt, Germany). An eluent with
171 0.1 mol/L sodium hydroxide and 0.01 mol/L sodium acetate was used with a flow rate of 0.5 mL/min.
172 Sugars were quantified by an amperometric detector. As byproducts of the isomerization reaction,
173 short-chain aldehydes and organic acids as well as furan compounds were considered. However, we
174 could not detect those compounds in any sample. The furan compounds hydroxymethylfurfural,
175 furfural and methylfurfural were separated at 20 °C in a Lichrospher 100 RP-18 column (Merck,
176 Darmstadt, Germany) and quantified by a UV detector at 290 nm. Therefore, a water–acetonitrile
177 eluent (9:1 v/v) at a flow rate of 1.4 mL/min was used. Short-chain aldehydes and organic acids like
178 formic acid, acetic acid, lactic acid and levulinic acid were separated with an Aminex HPX-87H
179 column (Biorad, Hercules, CA, USA) at a column temperature of 25 °C. The eluent was 0.004 mol/L
180 sulfuric acid at a flow rate of 0.65 mL/min. Detection was performed by RI and DAD.

181 In the experimental runs at neutral pH-conditions, glucose and fructose were also quantified by
182 an enzymatic test kit (Boehringer Mannheim/R Biopharm, Darmstadt, Germany). Quantification was
183 performed on a spectrophotometer CADAS 200 (Dr. Lange, Berlin, Germany).

184 The concentration of organic carbon (TOC) in the liquid samples was determined using a
185 Dimatoc 2000 (Dimatec Analysentechnik, Essen, Germany) applying the differential method. The
186 sample is catalytically oxidized at 850 °C, whereby all carbon is converted into CO₂, which is
187 measured with an IR detector. By adding phosphoric acid to the sample at 160 °C, only the inorganic
188 carbon is converted to CO₂ and subsequently measured.

189 The infrared spectra of dried hydrotalcite catalyst were recorded with a FT-IR spectrometer
190 660-IR (Varian, Palo Alto, USA) in transmittance mode for wavenumbers of 4000 - 400 cm⁻¹. The IR
191 spectroscopy was carried out using KBr pellets and obtained spectra were normalized.

192 The surface structures of dried catalyst were investigated via scanning electron microscopy
193 (SEM) in a LEO 982 Gemini (Carl Zeiss, Jena, Germany) equipped with a Schottky-type thermal field
194 emission cathode, secondary electron detectors (Everhart-Thornley, inlens), and a backscattered
195 electron detector.

196 For elemental analysis, the hydrotalcite catalyst is completely solved with concentrated acids
197 (HNO₃, HCl and HF in a volume ratio of 6:2:1). The microwave digestion takes place in a Multitwave
198 3000 (Anton Paar, Graz, Austria), where the heating power is increased linearly to 500 W over 15 min.
199 Then the temperature of 240 °C is maintained for 60 min. The analysis of the dissolved sample is
200 carried out using optical emission spectrometry with inductively coupled plasma in the radial
201 measurement mode on a 725 ICP-OES (Agilent, Santa Clara, CA, USA).

202 X-ray diffraction (XRD) provides information about the crystal structure of the dried catalyst.
203 The measurement is carried out for 60 min on a X'Pert Pro (PANalytical, Almelo, Netherlands). A
204 Bragg-Brentano arrangement with a copper anode and a nickel filter is used, the characteristic X-ray
205 radiation K_α being used for the measurement.

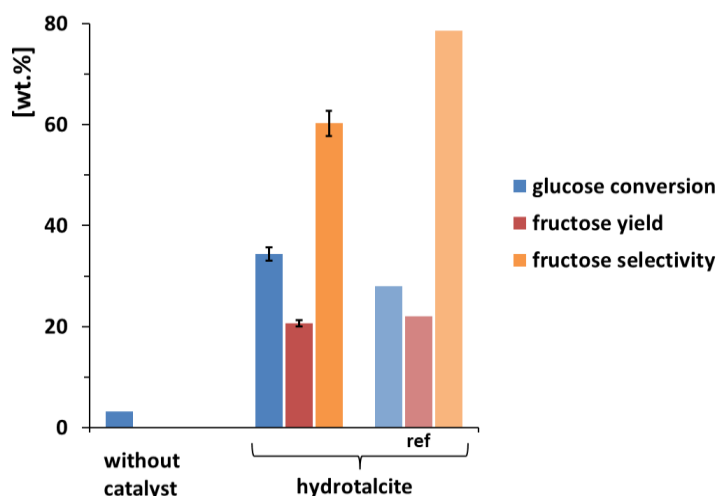
206 3. Results and discussion

207 3.1. Glucose isomerization under pH-neutral conditions

208 The isomerization of glucose solutions with hydrotalcite has already been performed, for
209 example by Lecomte et al. [15]. Under the same reaction conditions, similar fructose yields were
210 obtained (see Figure 2). However, the glucose conversion in this work (34 wt.%) is higher than by
211 Lecomte et al. [15] (27 wt.%), which mainly results from a different methodology for the calculation
212 of the conversion. Lecomte et al. [15] subtracted out the glucose that was adsorbed on the catalyst
213 (about 5 wt.%). Additionally, they identified mannose and psicose as by-products with a total yield
214 of not more than 5 wt.% [15]. In contrast, no mannose was detected in this study.

215 We used a different hydrotalcite catalyst than Lecomte et al. [15]. The Mg/Al ratio has a strong
216 effect on the catalytic properties for the isomerization reaction [24]. While the hydrotalcite used here
217 has a Mg/Al ratio of 3, Lecomte et al. [15] used a catalyst with a Mg/Al ratio of 4.5. The basicity is
218 highest at a Mg/Al ratio of 3 and decreases at lower as well as larger ratios [31]. Too high basicity can

219 lead to increased defragmentation reactions of the sugars to organic acids [17], which lowers the
 220 fructose selectivity. This was also shown by Moreau et al. [19], where a Mg/Al ratio of 3 led to a lower
 221 fructose selectivity than a Mg/Al ratio of 2.5.



222

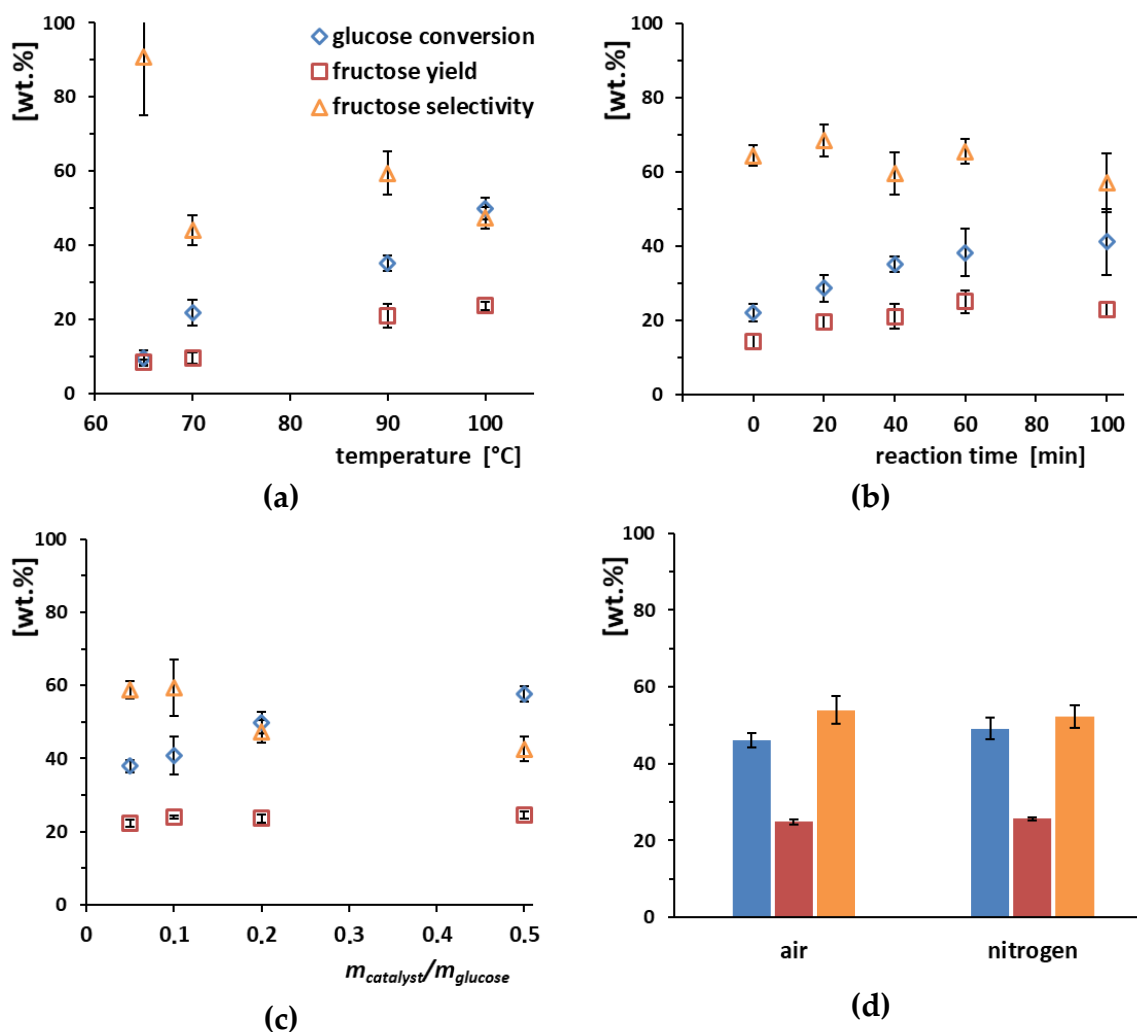
223 **Figure 2.** Glucose conversion and fructose yield using calcinated hydrotalcite, compared to Lecomte
 224 et al. [15] (ref), $C_{\text{glucose}} = 100 \text{ g/L}$, $T = 90 \text{ }^\circ\text{C}$, $t = 60 \text{ min}$, air atmosphere, $m_{\text{catalyst}}/m_{\text{glucose}} = 0.2$

225 Because the glucose concentrations after pretreatment of lignocellulose will be much lower than
 226 100 g/L, applied in the study of Lecomte et al. [15], parameter studies in this work are carried out
 227 with diluted glucose solutions. The variation in the isomerization temperature in the range from
 228 65 - 100 °C shows that, under mild reaction conditions of 65 °C, glucose can be selectively converted
 229 into fructose with hydrotalcite (see Figure 3 (a)). However, the yields are low (less than 10 wt.%).
 230 Higher temperatures lead to an increased glucose conversion, but the fructose selectivity decreases
 231 probably due to side reactions to unknown products, which lowers the fructose yield. However, no
 232 sugar defragmentation products (such as short-chain organic acids and aldehydes) or dehydration
 233 products (such as hydroxymethylfurfural and furfural) were detected via HPLC. Comparable studies
 234 with hydrotalcite found the sugar defragmentation products dihydroxyacetone, glycolaldehyde and
 235 lactic acid [16,18]. However, the applied residence times of 1.5-48 h were much longer than in this
 236 work. The concentrations of the defragmentation products are probably below the detection limit due
 237 to the shorter reaction time.

238 The glucose conversion increases with longer reaction time (see Figure 3 (b)). The fructose yield
 239 has a maximum of 25 wt.% at about 60 minutes. With longer reaction times, the fructose yield
 240 decreases again. Hence the fructose formed could have reacted to secondary products. As a result,
 241 undesirable side reactions of both glucose and fructose occur. Subsequent reactions of fructose with
 242 longer residence times were also found by Souza et al. [32] during isomerization with NaOH as
 243 catalyst.

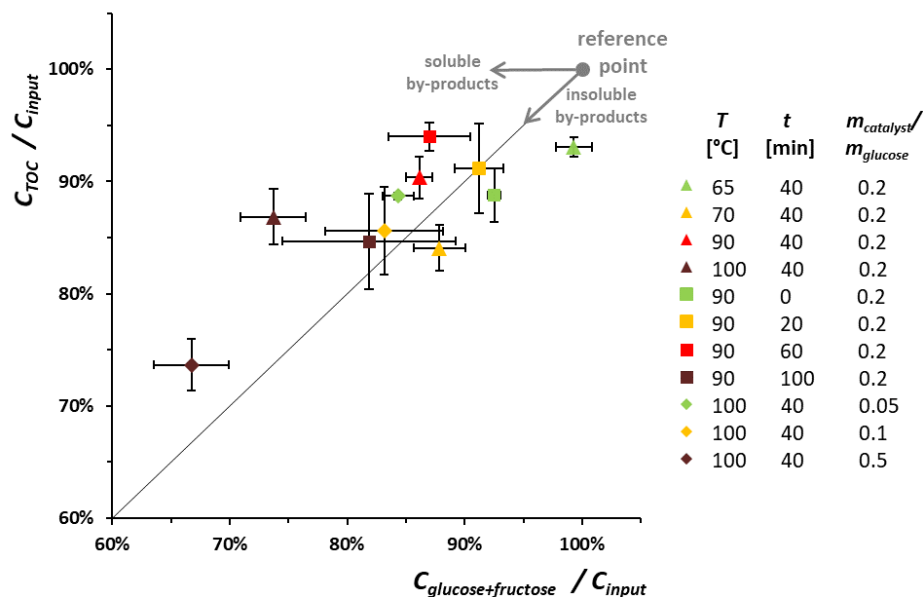
244 For the performed experiments, the mass ratio of catalyst to glucose has no influence on the
 245 fructose yield (see Figure 3 (c)). Thus, the number of active catalyst sites might not kinetically limit
 246 the isomerization reaction. The increase in the glucose conversion with a higher amount of catalyst
 247 suggests that glucose could deposit on the surface of the catalyst.

248 Whether the gas phase consists of air or nitrogen has no influence on the glucose conversion or
 249 the fructose yield (see Figure 3 (d)). Therefore, oxidation products with the ambient air play no role
 250 for the side reactions.



251 **Figure 3.** Glucose conversions and fructose yields using calcinated hydrotalcite with variation of
 252 (a) temperature, (b) reaction time, for $t = 0$ min sample is heated up to reaction temperature and then
 253 directly cooled down (c) mass ratio of catalyst to glucose at $T = 100$ °C and (d) gas atmosphere; always
 254 constant parameters: $c_{glucose} = 5$ g/L, $pH \approx 7$; parameters (unless otherwise stated): air atmosphere,
 255 $T = 90$ °C, $t = 40$ min, $m_{catalyst}/m_{glucose} = 0.2$

256 Because the glucose conversion is always much higher than the fructose yield, side reactions or
 257 deposition of glucose occur during isomerization. Figure 4 shows two carbon ratios to determine
 258 whether possible by-products are dissolved in the liquid phase. In the case of the reference point in
 259 Figure 4, no by-products are formed and the fructose selectivity is 100 wt.%. There are three model
 260 cases: (1) If the data point moves to the left in the diagram, by-products dissolved in water occur. (2)
 261 A shift of the data point on the bisector is caused by water-insoluble by-products. (3) If the data point
 262 is below the bisector, this is due to measurement errors. The experimental data from the isomerization
 263 cannot be clearly assigned to any of these three cases. However, most runs are closer to the bisector,
 264 which is associated with water-insoluble by-products. Either this could be deposits on the catalyst,
 265 or soluble polymers are formed under reaction conditions, which precipitate before sample analysis.
 266 The latter soluble polymers were reported by Souza et al. [32] as a by-product of isomerization. On
 267 the other hand, Souzanchia et al. [21] reported the formation of undesired insoluble by-products,
 268 mainly humins, on the surface of the used hydrotalcite catalysts.



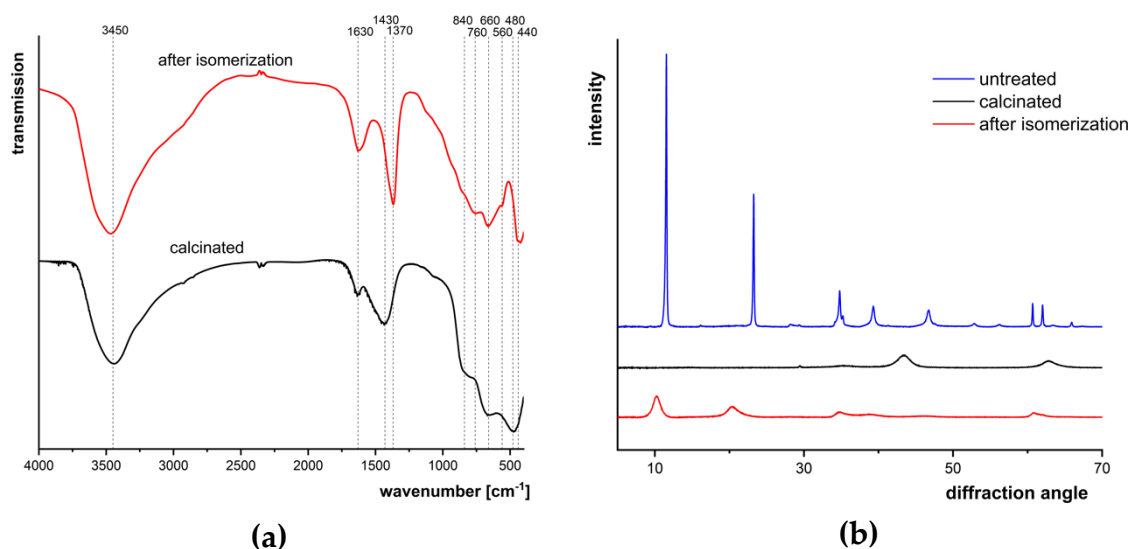
269

270 **Figure 4.** Carbon ratios for the isomerization of glucose with calcinated hydrotalcite; Y axis: TOC
 271 value of the product liquid to carbon input of the glucose solution C_{TOC}/C_{input} ; X axis: carbon of glucose
 272 and fructose in the product liquid to carbon input of the glucose solution $C_{glucose+fructose}/C_{input}$; reaction
 273 conditions: $C_{glucose} = 5$ g/L, $pH \approx 7$, air atmosphere

274 The IR spectra of the catalyst before and after the isomerization show only slight differences (see
 275 Figure 5 (a)). Both spectra are dominated by a broad O-H stretching vibration at 3450 cm^{-1} [33,34].
 276 The band at 1630 cm^{-1} is referred to O-H deformation vibrations [33]. The weak band at 760 cm^{-1} could
 277 be signals from Al-OH [33]. The bands in the range of $480 - 440\text{ cm}^{-1}$ are attributed to Mg-O-Al
 278 vibrations [33]. All other bands ($1430, 1370, 760, 660\text{ cm}^{-1}$) can originate from carbonates [29,33-35]. A
 279 precipitation of large amounts of organic matter during the isomerization on the catalyst surface
 280 is not detectable by IR spectroscopy, because no vibrations of organic compounds are found. For
 281 example, the spectra of the catalyst after isomerization show neither C-H valence vibrations at
 282 2900 cm^{-1} , nor C=C valence vibrations of aromatics at $1600 - 1500\text{ cm}^{-1}$.

283 XRD is also used to characterize the catalyst (see Figure 5 (b)). In the untreated hydrotalcite two
 284 sharp, symmetrical signals occur at 11.5° and 23.2° with high intensity. Weaker signals can be found
 285 at $34.8; 39.8; 46.7; 60.7$ and 62.0° . The sharp XRD signals show that the untreated hydrotalcite catalyst
 286 has a crystalline structure and can be used to characterize the layered crystal structure [36,37]. The
 287 diffraction angles of the commercially available hydrotalcite used here are identical to other
 288 synthesized hydrotalcites [16,17,29,33].

289 After calcining the hydrotalcite, all XRD signals of the layered crystal structure have
 290 disappeared. So, the crystalline structure has been lost and disordered Mg-Al mixed oxides have
 291 formed [17,29,38]. After the isomerization, part of the crystalline order in the hydrotalcite returns,
 292 which can be seen from the XRD signals at low diffraction angles. This could be achieved by
 293 rehydration of the catalyst with water from the isomerization solution, whereby the layered crystal
 294 structure is restored by the “memory effect” [17,29,38].



295 **Figure 5.** (a) IR spektra and (b) XRD pattern of hydrotalcite; reaction conditions: $C_{\text{glucose}} = 5 \text{ g/L}$, $pH \approx 7$,
 296 air atmosphere, $T = 100 \text{ }^\circ\text{C}$, $t = 40 \text{ min}$, $m_{\text{catalyst}}/m_{\text{glucose}} = 0.2$

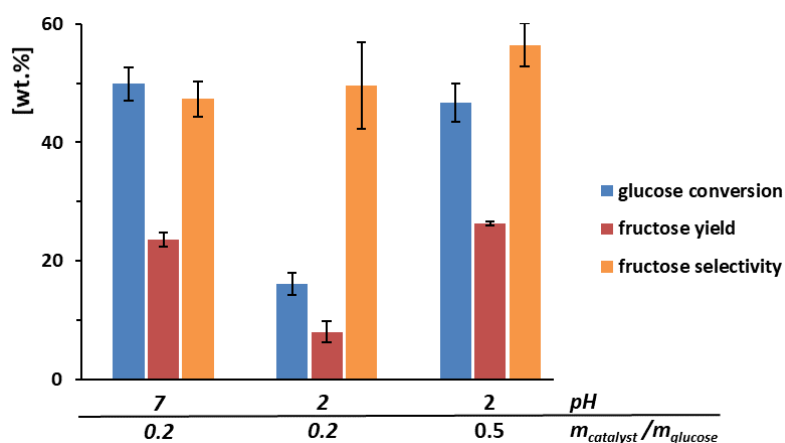
297 3.2. Glucose isomerization under pH-acidic conditions

298 By now, isomerization with hydrotalcite has only been investigated under pH-neutral reaction
 299 conditions. However, the hydrolyzate from the acid-catalyzed hydrolysis of lignocellulose is
 300 produced with an acidic pH-value. Therefore, it is investigated here, whether the hydrotalcite
 301 catalyzes the isomerization even under acidic conditions. As can be seen in Figure 6, the glucose
 302 conversion drops sharply, if the pH value is decreased. This effect can be compensated by a larger
 303 mass ratio of catalyst to glucose.

304 In addition, the dissolved metal ions in the product liquid are analyzed. During the
 305 isomerization, especially magnesium ions are released from the catalyst. For example, 3.2 wt.% of the
 306 magnesium bound in the hydrotalcite goes into solution, in the run shown in Figure 6 with
 307 $m_{\text{catalyst}}/m_{\text{glucose}} = 0.5$. In contrast, aluminum remains almost completely in the solid.

308 Under acidic pH conditions, hydrotalcite loses its activity for isomerization, which can be
 309 concluded from the decreased glucose conversion at $pH = 2$. The anions in the hydrotalcite solid
 310 structure are OH^- ions after calcination and subsequent suspension in water [15]. These hydroxides
 311 are neutralized with the hydronium ions of sulfuric acid. This also makes the metal cations partially
 312 water-soluble.

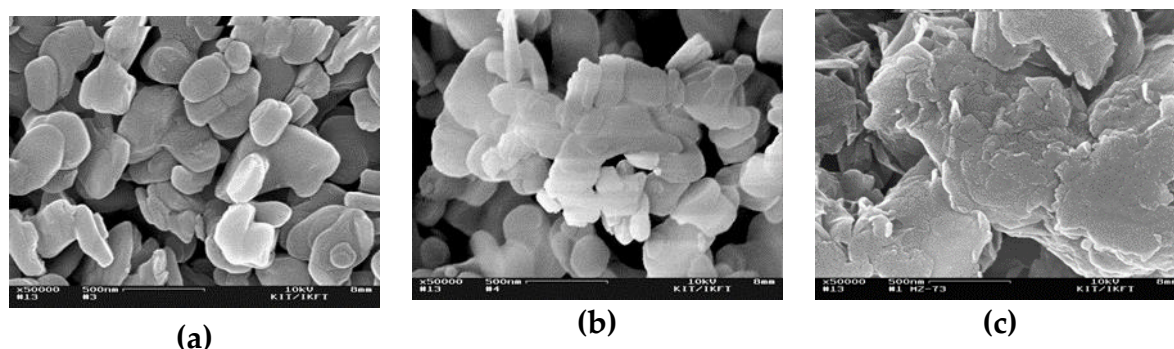
313



314

315 **Figure 6.** Glucose conversions and fructose yields with calcinated hydrotalcite with variation of the
 316 pH value by adding sulfuric acid, constant parameters $C_{\text{glucose}} = 5 \text{ g/L}$, air atmosphere, $T = 100 \text{ }^\circ\text{C}$,
 317 $t = 40 \text{ min}$

318 After the isomerization under acidic pH conditions, a clear change in the catalyst morphology is
 319 visible (see Figure 7). The catalyst appears to have partially dissolved and re-agglomerated into new
 320 particles of different morphology. The particles after the isomerization reaction are much larger than
 321 the particles of the calcinated catalyst before the start of the reaction.
 322



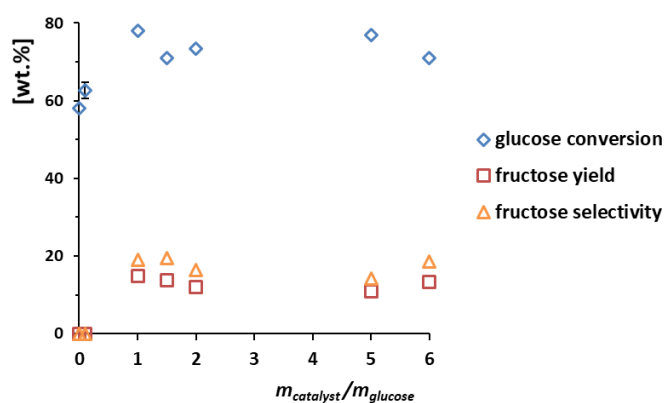
323 **Figure 7.** SEM images of the catalyst hydrotalcite in 50,000x (a) before calcination, (b) calcinated and
 324 (c) after isomerization; reaction conditions: $T = 100\text{ }^{\circ}\text{C}$, $t = 40\text{ min}$, $pH = 2$, air atmosphere,
 325 $m_{\text{catalyst}}/m_{\text{glucose}} = 0.2$

326 3.3. Isomerization of hydrolyzate from lignocellulose without previous neutralization

327 If the acidic hydrolyzate is exposed to the typical reaction conditions ($100\text{ }^{\circ}\text{C}$, 60 min) of the
 328 isomerization without the addition of hydrotalcite catalyst, no fructose is produced but almost
 329 60 wt.% of the dissolved glucose is converted (see Figure 8). This shows that the organic compounds
 330 in the hydrolyzate are very reactive in a pH-acidic medium.

331 When hydrotalcite is added in a catalyst/glucose ratio of 0.1, no fructose is formed. In contrast,
 332 in the case of pH-neutral glucose solutions, this catalyst loading was sufficient for fructose formation
 333 (see Figure 3 (c)). Presumably, the catalytic active OH^- ions in the hydrotalcite structure are
 334 neutralized by the sulfuric acid from the hydrolyzate, as discussed in the previous chapter. The
 335 alkaline structure of the catalyst is lost and the isomerization can no longer be catalyzed. This
 336 neutralization effect of the catalyst can be compensated by offering hydrotalcite in excess. However,
 337 using the isomerization catalyst as a neutralizing agent is not useful. Rather, the hydrolyzate should
 338 be neutralized before the isomerization by an inexpensive base.

339 Fructose is formed at a mass ratio of catalyst to glucose of 1 (see Figure 8). Even if this ratio is
 340 increased further, the fructose yield remains relatively constant at around 11 - 15 wt.%. In general,
 341 these fructose yields of the hydrolyzate are lower than the results with glucose solutions. In addition,
 342 the glucose turnover in the hydrolyzate is much higher compared to a glucose solution.
 343



344

345 **Figure 8.** Glucose conversions and fructose yields of the calcinated hydrolyzate from lignocellulose
 346 with varying mass ratio of hydrotalcite catalyst to glucose; pretreatment parameters: beech wood,

347 $T = 180\text{ }^{\circ}\text{C}$, $0.05\text{ mol/L H}_2\text{SO}_4$; isomerization parameters: $C_{\text{glucose}} = 2.5\text{ g/L}$, air atmosphere, $T = 100\text{ }^{\circ}\text{C}$, $t =$
348 60 min , $\text{pH} = 1.3$

349 3.4. Isomerization of hydrolyzate from lignocellulose after previous neutralization

350 The two Brønsted bases NaOH and Ba(OH)₂ are used to neutralize the hydrolyzate from the
351 sulfuric acid-catalyzed pretreatment of lignocellulose. When the pH is adjusted to 7, the hydrolyzate
352 changes color from light brown to dark brown for both neutralizing agents. While the neutralization
353 product Na₂SO₄ is highly water-soluble, BaSO₄ is almost insoluble (2.3 mg/L [39]). Therefore, a
354 precipitate is formed in the hydrolyzate immediately after addition of Ba(OH)₂. This difference in
355 solubility and its effect on the process was the reason to use Ba(OH)₂ as well as NaOH.

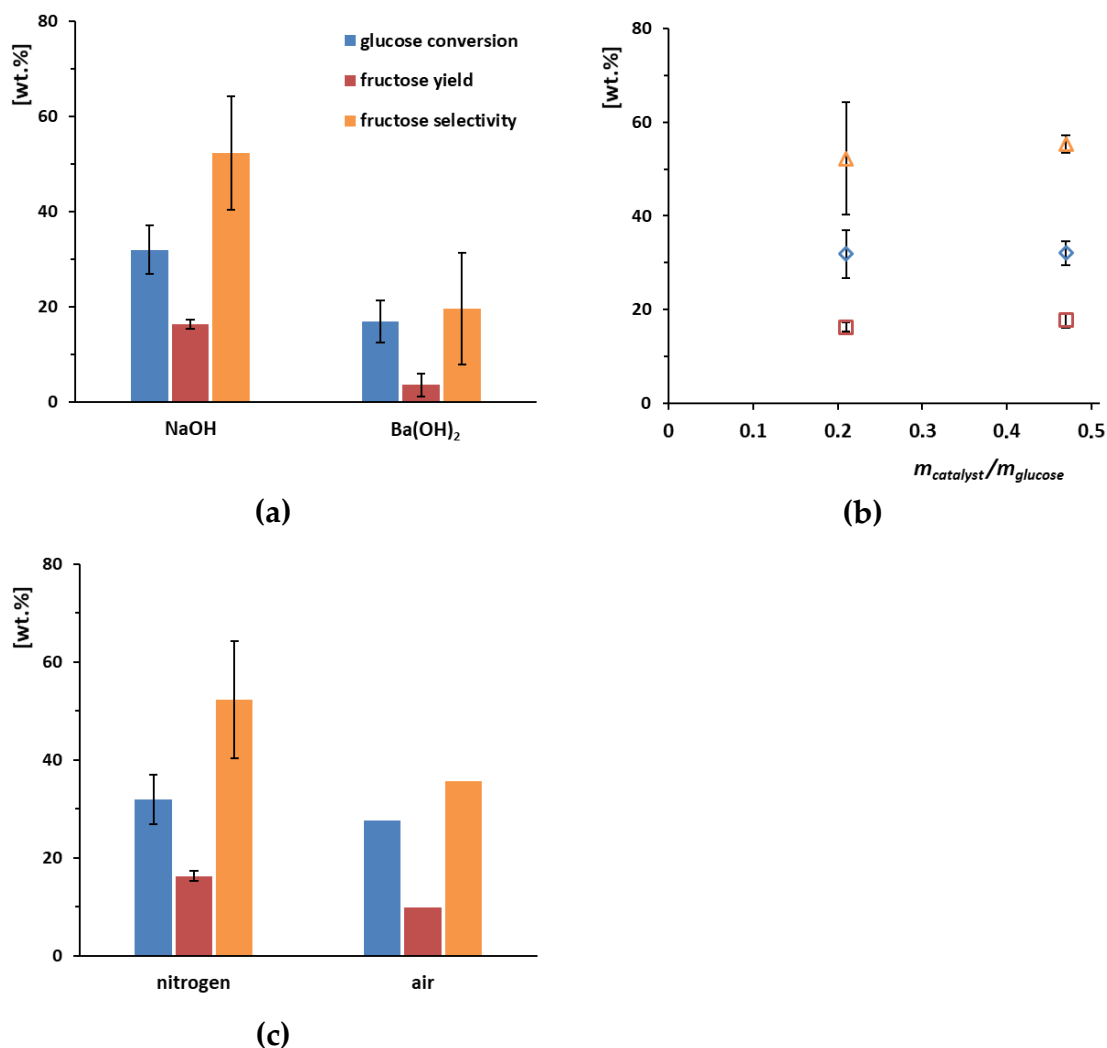
356 The organic compounds remain largely dissolved in both neutralization variants. The analysis
357 of the carbon concentration before and after neutralization shows a recovery of 91.7 % for NaOH and
358 97.6 % for Ba(OH)₂. In addition, concentrations of measured byproducts from acid-catalyzed
359 pretreatment of lignocellulose (hydroxymethylfurfural, furfural, levulinic acid, formic acid and acetic
360 acid) were identical before and after neutralization step. The solid precipitate of the Ba(OH)₂
361 neutralization is examined via IR spectroscopy and shows agreement with the typical IR bands of
362 BaSO₄, while typical bands of organic compounds are not dominant (data not shown). So, if a salt is
363 precipitated by the neutralization, no larger amounts of organic matter adsorb on it or co-precipitate.

364 No measurable fructose yields can be achieved with neutralized hydrolyzate, when a
365 hydrotalcite catalyzed isomerization at mild reaction conditions of 60 °C and 40 min is performed.
366 However, fructose is obtained if the temperature is increased to 100 °C (see Figure 9). The mass ratio
367 of catalyst to glucose in the examined range of 0.2 to 0.5 has no strong influence on the isomerization
368 (see Figure 9 (b)). If isomerization takes place under inert gas, the fructose yield seems higher than
369 with ambient air (see Figure 9 (c)). When the hydrolyzate is neutralized with NaOH before
370 isomerization step, a much higher fructose yield can be achieved, compared to neutralization with
371 Ba(OH)₂ (see Figure 9 (a)). Using NaOH, the formed sodium sulfate salts remain solved in the
372 isomerization step, whereas barium sulfate precipitates and is therefore not present in the
373 isomerization step. The presence either of the Na⁺ ions or the sulfate ions in the hydrolyzate appear
374 to have a positive effect on the isomerization, which should be addressed in further studies.

375 The concentrations of byproducts from acid-catalyzed pretreatment of lignocellulose changed
376 during isomerization. For example, following concentration changes occurred using nitrogen
377 atmosphere, NaOH neutralization and $m_{\text{catalyst}}/m_{\text{glucose}} = 0.21$ with conditions listed in Figure 9:
378 Hydroxymethylfurfural (910 mg/L decreased to 710 mg/L), furfural (230 mg/L decreased to 50 mg/L),
379 levulinic acid (50 mg/L increased to 610 mg/L), formic acid (30 mg/L increased to 260 mg/L) and
380 acetic acid (30 mg/L increased to 160 mg/L). Thus, considerable amounts of organic acids are formed
381 during isomerization step of biomass-derived hydrolyzate, whereas hydroxymethylfurfural and
382 furfural could be partly converted or adsorb on the catalyst surface.

383 By neutralizing the hydrolyzate before the isomerization step, it was possible to reduce the ratio
384 of glucose conversions to by-products drastically. Using a pH-acidic hydrolyzate, 60-80 wt.% of
385 glucose are converted while maximal 15 wt.% fructose being formed (see Figure 8). On the other
386 hand, after prior neutralization, the glucose conversion is reduced to 32 wt.% and a fructose yield of
387 16 wt.% is achieved (see Figure 9). The previous neutralization presumably prevents acid-catalyzed
388 side reactions of the glucose, which take place during the isomerization step under acidic conditions
389 (e.g. fragmentation reactions). When the just mentioned isomerization results of neutralized
390 lignocellulose hydrolyzate are compared with glucose standard solutions, a higher fructose yield is
391 obtained with glucose standard solution under the same reaction conditions (23 wt.% fructose yield
392 at 41 wt.% glucose conversion, see Figure 3). Further studies should show, if these differences are due
393 to deactivation of the catalyst using the neutralized hydrolyzate. For example, the role of
394 (1) byproducts from acid-catalyzed pretreatment of lignocellulose (other sugars, furfural,
395 hydroxymethylfurfural, organic acids, high-molecular-weight humins) as well as (2) salts from
396 pretreatment catalyst and neutralization agent should be investigated. In addition, the recovery and

397 regeneration of hydrotalcite catalyst after isomerization of hydrolyzate from lignocellulose
 398 pretreatment should be addressed.
 399



400 **Figure 9.** Glucose conversions and fructose yields of the neutralized hydrolyzate from lignocellulose
 401 with variation of (a) neutralizing agent, (b) mass ratio of calcinated hydrotalcite catalyst to glucose
 402 and (c) gas atmosphere; pretreatment parameters: spruce wood, $T = 200\text{ }^{\circ}\text{C}$, $0.05\text{ mol/L H}_2\text{SO}_4$;
 403 constant isomerization parameters: $c_{glucose} = 2.1\text{ g/L}$, $pH \approx 7$, $T = 100\text{ }^{\circ}\text{C}$, $t = 40\text{ min}$; parameters (unless
 404 otherwise stated): neutralization with NaOH, nitrogen atmosphere, $m_{catalyst}/m_{glucose} = 0.21$

405 4. Conclusions

406 Parameter studies with glucose solutions under pH-neutral conditions show the best
 407 isomerization results (25 wt.% fructose yield, 38 wt.% glucose conversion) at a mass ratio of
 408 hydrotalcite to glucose of 0.2 at $90\text{ }^{\circ}\text{C}$ for 60 min reaction time. Carbon balance suggests that side
 409 products are more likely water-insoluble.

410 Under acidic pH conditions, the hydrotalcite loses its activity for isomerization. The hydroxides
 411 in the solid structure are neutralized by hydronium ions in solution. Thereby the metal cations
 412 become partially water-soluble too and the morphology of the catalyst is altered. In consequence, it
 413 is unavoidable to neutralize the acidic hydrolyzate before the isomerization step with an inexpensive
 414 base. During neutralization, almost all organic compounds stay in the liquid state. As a neutralizing
 415 agent NaOH is preferred over Ba(OH)₂, since better fructose yields are achieved with NaOH (16 wt.%
 416 fructose yield, 32 wt.% glucose conversion).

417 The isomerization of glucose-containing hydrolyzates to fructose is a key step in the process
 418 from lignocellulosic biomass to the platform chemical HMF. The catalytic system should be better

419 understood, especially the occurring side reactions. If the yields of side products are known, the
420 carbon balance can be improved. Besides studies of the catalytic system with pure model compounds,
421 especially the application to real biomass-derived samples like hydrolyzates should be enhanced.
422

423 **Author Contributions:** D.S., A.Kl., S.W. and M.Z. designed and performed the experiments as well as analyzed
424 the data. D.S., S.W., A.Kr. and J.S. wrote the article.

425 **Funding:** This work was financially supported by the German Federal Ministry of Food, Agriculture and
426 Consumer Protection (FNR project number 22027811) based on a decision of the German Bundestag. We
427 acknowledge support by Deutsche Forschungsgemeinschaft and Open Access Publishing Fund of Karlsruhe
428 Institute of Technology.

429 **Acknowledgments:** We thank Ines Budei for her experimental work. Matthias Pagel and Thomas Tietz built the
430 pretreatment reactor. We thank Sonja Habicht and Armin Lautenbach for HPLC sugar analysis, Dr. Manuel
431 Gentzen for XRD measurement, Hermann Köhler for ICP-OES and Wilhelm Habicht for SEM measurements.
432 We acknowledge Prof. Dr. Nicolaus Dahmen for project supervision.

433 **Conflicts of Interest:** The authors declare no conflict of interest. The founding sponsors had no role in the design
434 of the study; in the collection, analyses, or interpretation of data; in the writing of the manuscript, and in the
435 decision to publish the results.

436 References

- 437 1. Steinbach, D.; Kruse, A.; Sauer, J. Pretreatment technologies of lignocellulosic biomass in water in view
438 of furfural and 5-hydroxymethylfurfural production - A review. *Biomass Conversion and Biorefinery* **2017**,
439 *7*, 247-274, doi:10.1007/s13399-017-0243-0.
- 440 2. van Putten, R.J.; van der Waal, J.C.; de Jong, E.; Rasrendra, C.B.; Heeres, H.J.; de Vries, J.G.
441 Hydroxymethylfurfural, a versatile platform chemical made from renewable resources. *Chem Rev* **2013**,
442 *113*, 1499-1597, doi:10.1021/Cr300182k.
- 443 3. Steinbach, D.; Kruse, A.; Sauer, J.; Vetter, P. Sucrose Is a Promising Feedstock for the Synthesis of the
444 Platform Chemical Hydroxymethylfurfural. *Energies* **2018**, *11*, 645.
- 445 4. Bhosale, S.H.; Rao, M.B.; Deshpande, V.V. Molecular and industrial aspects of glucose isomerase.
446 *Microbiol Rev* **1996**, *60*, 280-+, doi:Doi 10.1128/Mmbr.60.2.280-300.1996.
- 447 5. Tewari, Y.B. Thermodynamics of industrially-important, enzyme-catalyzed reactions. *Appl Biochem*
448 *Biotech* **1990**, *23*, 187-203, doi:10.1007/bf02942054.
- 449 6. Roman-Leshkov, Y.; Moliner, M.; Labinger, J.A.; Davis, M.E. Mechanism of Glucose Isomerization
450 Using a Solid Lewis Acid Catalyst in Water. *Angew Chem Int Edit* **2010**, *49*, 8954-8957,
451 doi:10.1002/anie.201004689.
- 452 7. Bermejo-Deval, R.; Assary, R.S.; Nikolla, E.; Moliner, M.; Román-Leshkov, Y.; Hwang, S.-J.; Palsdottir,
453 A.; Silverman, D.; Lobo, R.F.; Curtiss, L.A., et al. Metalloenzyme-like catalyzed isomerizations of sugars
454 by Lewis acid zeolites. *Proceedings of the National Academy of Sciences of the United States of America* **2012**,
455 *109*, 9727-9732, doi:10.1073/pnas.1206708109.
- 456 8. Allen, K.N.; Lavie, A.; Farber, G.K.; Glasfeld, A.; Petsko, G.A.; Ringe, D. Isotopic Exchange plus
457 Substrate and Inhibition Kinetics of D-Xylose Isomerase Do Not Support a Proton-Transfer Mechanism.
458 *Biochemistry* **1994**, *33*, 1481-1487, doi:10.1021/bi00172a026.
- 459 9. Kovalevsky, A.Y.; Hanson, L.; Fisher, S.Z.; Mustyakimov, M.; Mason, S.A.; Trevor Forsyth, V.; Blakeley,
460 M.P.; Keen, D.A.; Wagner, T.; Carrell, H.L., et al. Metal Ion Roles and the Movement of Hydrogen
461 during Reaction Catalyzed by D-Xylose Isomerase: A Joint X-Ray and Neutron Diffraction Study.
462 *Structure* **2010**, *18*, 688-699, doi:10.1016/j.str.2010.03.011.

- 463 10. Usuki, C.; Kimura, Y.; Adachi, S. Isomerization of Hexoses in Subcritical Water. *Food Science and*
464 *Technology Research* **2007**, *13*, 205-209, doi:10.3136/fstr.13.205.
- 465 11. Delidovich, I.; Palkovits, R. Catalytic Isomerization of Biomass-Derived Aldoses: A Review.
466 *Chemsuschem* **2016**, *9*, 547-561, doi:10.1002/cssc.201501577.
- 467 12. Li, B.; Li, L.; Zhang, Q.; Weng, W.; Wan, H. Attapulgite as natural catalyst for glucose isomerization to
468 fructose in water. *Catal Commun* **2017**, *99*, 20-24, doi:10.1016/j.catcom.2017.05.011.
- 469 13. Marianou, A.A.; Michailof, C.M.; Pineda, A.; Iliopoulou, E.F.; Triantafyllidis, K.S.; Lappas, A.A. Glucose
470 to Fructose Isomerization in Aqueous Media over Homogeneous and Heterogeneous Catalysts.
471 *Chemcatchem* **2016**, *8*, 1100-1110, doi:10.1002/cctc.201501203.
- 472 14. Cantrell, D.G.; Gillie, L.J.; Lee, A.F.; Wilson, K. Structure-reactivity correlations in MgAl hydrotalcite
473 catalysts for biodiesel synthesis. *Applied Catalysis A: General* **2005**, *287*, 183-190,
474 doi:10.1016/j.apcata.2005.03.027.
- 475 15. Lecomte, J.; Finiels, A.; Moreau, C. Kinetic study of the isomerization of glucose into fructose in the
476 presence of anion-modified hydrotalcites. *Starch-Starke* **2002**, *54*, 75-79, doi:10.1002/1521-
477 379x(200202)54:2<75::Aid-Star75>3.0.Co;2-F.
- 478 16. Delidovich, I.; Palkovits, R. Structure-performance correlations of Mg-Al hydrotalcite catalysts for the
479 isomerization of glucose into fructose. *Journal of Catalysis* **2015**, *327*, 1-9, doi:10.1016/j.jcat.2015.04.012.
- 480 17. Yu, S.; Kim, E.; Park, S.; Song, I.K.; Jung, J.C. Isomerization of glucose into fructose over Mg-Al
481 hydrotalcite catalysts. *Catal Commun* **2012**, *29*, 63-67, doi:10.1016/j.catcom.2012.09.015.
- 482 18. Delidovich, I.; Palkovits, R. Catalytic activity and stability of hydrophobic Mg-Al hydrotalcites in the
483 continuous aqueous-phase isomerization of glucose into fructose. *Catal Sci Technol* **2014**, *4*, 4322-4329,
484 doi:10.1039/c4cy00776j.
- 485 19. Moreau, C.; Durand, R.; Roux, A.; Tichit, D. Isomerization of glucose into fructose in the presence of
486 cation-exchanged zeolites and hydrotalcites. *Appl Catal a-Gen* **2000**, *193*, 257-264, doi:10.1016/S0926-
487 860x(99)00435-4.
- 488 20. Weisgerber, L.; Palkovits, S.; Palkovits, R. Development of a reactor setup for continuous dehydration
489 of carbohydrates. *Chem-Ing-Tech* **2013**, *85*, 512-515, doi:10.1002/cite.201200203.
- 490 21. Souzanchi, S.; Nazari, L.; Rao, K.T.V.; Yuan, Z.; Tan, Z.; Xu, C. Catalytic isomerization of glucose to
491 fructose using heterogeneous solid Base catalysts in a continuous-flow tubular reactor: Catalyst
492 screening study. *Catal Today* **2019**, *319*, 76-83, doi:10.1016/j.cattod.2018.03.056.
- 493 22. Yabushita, M.; Shibayama, N.; Nakajima, K.; Fukuoka, A. Selective Glucose-to-Fructose Isomerization
494 in Ethanol Catalyzed by Hydrotalcites. *Acs Catal* **2019**, *9*, 2101-2109, doi:10.1021/acscatal.8b05145.
- 495 23. Lee, G.; Kang, J.Y.; Yan, N.; Suh, Y.-W.; Jung, J.C. Simple preparation method for Mg-Al hydrotalcites
496 as base catalysts. *Journal of Molecular Catalysis A: Chemical* **2016**, *423*, 347-355,
497 doi:10.1016/j.molcata.2016.07.018.
- 498 24. Kang, J.; Lee, G.; Suh, Y.-W.; Jung, J. Effect of Mg/Al Atomic Ratio of Mg-Al Hydrotalcites on Their
499 Catalytic Properties for the Isomerization of Glucose to Fructose. *Journal of Nanoscience and*
500 *Nanotechnology* **2017**, *17*, 8242-8247, doi:10.1166/jnn.2017.15081.
- 501 25. Park, S.; Kwon, D.; Kang, J.Y.; Jung, J.C. Influence of the preparation method on the catalytic activity of
502 MgAl hydrotalcites as solid base catalysts. *Green Energy & Environment* **2019**, *4*, 287-292,
503 doi:10.1016/j.gee.2018.11.003.

- 504 26. Murzin, D.Y.; Murzina, E.V.; Aho, A.; Kazakova, M.A.; Selyutin, A.G.; Kubicka, D.; Kuznetsov, V.L.;
505 Simakova, I.L. Aldose to ketose interconversion: galactose and arabinose isomerization over
506 heterogeneous catalysts. *Catal Sci Technol* **2017**, *7*, 5321-5331, doi:10.1039/c7cy00281e.
- 507 27. Upare, P.P.; Chamas, A.; Lee, J.H.; Kim, J.C.; Kwak, S.K.; Hwang, Y.K.; Hwang, D.W. Highly Efficient
508 Hydrotalcite/1-Butanol Catalytic System for the Production of the High-Yield Fructose Crystal from
509 Glucose. *ACS Catal* **2020**, *10*, 1388-1396, doi:10.1021/acscatal.9b01650.
- 510 28. Antal, M.J.; Mok, W.S.L.; Richards, G.N. Mechanism of formation of 5-(hydroxymethyl)-2-furaldehyde
511 from d-fructose and sucrose. *Carbohydr Res* **1990**, *199*, 91-109, doi:10.1016/0008-6215(90)84096-D.
- 512 29. Asghari, F.S.; Yoshida, H. Acid-catalyzed production of 5-hydroxymethyl furfural from D-fructose in
513 subcritical water. *Ind Eng Chem Res* **2006**, *45*, 2163-2173, doi:10.1021/ie051088y.
- 514 30. Świątek, K.; Gaag, S.; Klier, A.; Kruse, A.; Sauer, J.; Steinbach, D. Acid Hydrolysis of Lignocellulosic
515 Biomass: Sugars and Furfurals Formation. *Catalysts* **2020**, *10*, 437, doi:10.3390/catal10040437.
- 516 31. Xie, W.; Peng, H.; Chen, L. Calcined Mg–Al hydrotalcites as solid base catalysts for methanolysis of
517 soybean oil. *Journal of Molecular Catalysis A: Chemical* **2006**, *246*, 24-32, doi:10.1016/j.molcata.2005.10.008.
- 518 32. Souza, R.O.L.; Fabiano, D.P.; Feche, C.; Rataboul, F.; Cardoso, D.; Essayem, N. Glucose-fructose
519 isomerisation promoted by basic hybrid catalysts. *Catal Today* **2012**, *195*, 114-119,
520 doi:10.1016/j.cattod.2012.05.046.
- 521 33. Wiyantoko, B.; Kurniawati, P.; Purbaningties, T.E.; Fatimah, I. Synthesis and Characterization of
522 Hydrotalcite at Different Mg/Al Molar Ratios. *Procedia Chemistry* **2015**, *17*, 21-26,
523 doi:10.1016/j.proche.2015.12.115.
- 524 34. Hernandez-Moreno, M.J.; Ulibarri, M.A.; Rendon, J.L.; Serna, C.J. IR characteristics of hydrotalcite-like
525 compounds. *Physics and Chemistry of Minerals* **1985**, *12*, 34-38, doi:10.1007/bf00348744.
- 526 35. Frost, R.L.; Scholz, R.; López, A.; Theiss, F.L. Vibrational spectroscopic study of the natural layered
527 double hydroxide manasseite now defined as hydrotalcite-2H – Mg₆Al₂(OH)₁₆[CO₃]₄·4H₂O.
528 *Spectrochimica Acta Part A: Molecular and Biomolecular Spectroscopy* **2014**, *118*, 187-191,
529 doi:10.1016/j.saa.2013.08.105.
- 530 36. Cavani, F.; Trifirò, F.; Vaccari, A. Hydrotalcite-type anionic clays: Preparation, properties and
531 applications. *Catal Today* **1991**, *11*, 173-301, doi:10.1016/0920-5861(91)80068-K.
- 532 37. Pérez-Ramírez, J.; Abelló, S.; van der Pers, N.M. Influence of the Divalent Cation on the Thermal
533 Activation and Reconstruction of Hydrotalcite-like Compounds. *The Journal of Physical Chemistry C*
534 **2007**, *111*, 3642-3650, doi:10.1021/jp064972q.
- 535 38. Pérez-Ramírez, J.; Abelló, S.; van der Pers, N.M. Memory Effect of Activated Mg–Al Hydrotalcite: In
536 Situ XRD Studies during Decomposition and Gas-Phase Reconstruction. *Chemistry – A European Journal*
537 **2007**, *13*, 870-878, doi:10.1002/chem.200600767.
- 538 39. Bageri, B.S.; Mahmoud, M.A.; Shawabkeh, R.A.; Abdurhaem, A. Evaluation of Barium Sulfate (Barite)
539 Solubility Using Different Chelating Agents at a High Temperature. *Journal of Petroleum Science and*
540 *Technology* **2017**, *7*, 42-56, doi:10.22078/jpst.2017.707.
- 541

